Development of a Low Profile Conformal UHF RFID Tag Antenna for Identification of Water Bottles

Toni Björninen, Leena Ukkonen, Lauri Sydänheimo
Rauma Research Unit of the Department of Electronics
Tampere University of Technology
26100 Rauma, Finland
toni.bjorninen@tut.fi

Atef Z. Elsherbeni
Department of Electrical Engineering
The University of Mississippi
University, MS 38677, USA
atef@olemiss.edu

***Abstract*—Development of a low profile conformal RFID tag antenna with an omnidirectional pattern when mounted on a water bottle is discussed. Results from full-wave electromagnetic simulations are presented to explain the design procedure and to evaluate the performance of the prototype tag antenna. The design uncertainty is quantified based on the expected maximum variations in the tag antenna and tag chip impedances. Wireless measurements based on the EPC Generation 2 protocol are used in experimental tag design verification. The prototype tag achieves more than two-meter maximum line of sight read range for 866.6 MHz to 954.2 MHz frequency band.**

***Index Terms*—Radio Frequency Identification (RFID), RFID tag antennas, Conformal antennas, UHF antennas**

I. INTRODUCTION

Versatile and energy efficient passive radio frequency identification (RFID) technology is a strong candidate to replace some of the present automatic identification systems, based on the visual line of sight connection, such as bar-code, machine vision and biometric identification, or using active transmitters to track assets.

Currently, the functionality of RFID technology is already expanding beyond the identification for asset tracking and supply chain management [1] to include wireless sensor capabilities [2], which provide quality control and safety. Applications of body monitoring and tracking of people with wearable RFID are also emerging [3]-[4]. However, there are still unresolved challenges related to design of cost effective RFID tag antennas for the identification of objects consisting of materials that are unfavorable for the operation of antennas. Pronounced examples include objects containing metals or lossy aquatic liquids. In addition, mounting the tag on a non-planar surface may change its radiation properties and this need to be accounted for in the design [5]. Nonetheless, objects with various shapes and unfavorable materials for antennas are encountered continually in practical applications. It is therefore important to explore tag antenna design approaches further to guarantee reliable identification for these objects as well.

In this study, a low profile UHF RFID tag antenna mountable directly onto a cylindrical water bottle is developed. The design challenges discussed include achieving sufficient antenna radiation efficiency with an omnidirectional pattern in the close vicinity of the water using a single conformal layer antenna structure.

This research work was funded by the Finnish Funding Agency for Technology and Innovation (TEKES), Academy of Finland, Centennial Foundation of Finnish Technology Industries, Tampere Doctoral Programme in Information Science and Engineering (TISE), HPY Research Foundation, and Nokia Foundation.

II. TAG ANTENNA DESIGN

A. Concept and Requirements

The electromagnetic properties of the materials in contact or in the vicinity of the antenna conductor affect the current distribution in the conductor. This is due to the interaction between the material and electromagnetic field created by the antenna current. The physical mechanisms of the interaction are polarization and magnetization of the material, energy dissipation in these processes, as well as in conduction current created in the material. Consequently, the antenna input impedance and radiation properties are affected.

Compared with many solid state materials, water has high permittivity and considerable electrical conductivity at microwave frequencies and therefore strong interaction with a nearby tag antenna is expected. To account for the influence of water on the antenna, a co-design approach where the water bottle is considered a part of the antenna was taken in this study. The material parameters of water used in the design are $\varepsilon_{r,water}$=79.2 and σ_{water}=0.267 S/m for pure water at 1 GHz at the temperature of 20 C° reported by Ellison et al. [6]. Combining these data, gives the loss tangent $\tan\delta_{water}$=0.061 at 1 GHz.

Typical design constraints for RFID tag antennas aimed for the item level identification of a very large asset base are low manufacturing costs, operation over the global UHF RFID frequencies and, very often, seamless integration of the tag antennas to the objects to be identified. One example of this type of application is the identification of water bottles and considering the above requirements, a suitable tag consists of a single conductor layer on a thin low cost substrate material, with no added discrete components other than the RFID IC.

B. Design process and simulation results

The design process outlined in this section is based on the finite element method (FEM) simulations using Ansoft's high

frequency structure simulator (HFSS). Materials included in the simulation model are, in addition to the water, the plastic used in the bottle and the antenna platform material, which is a thin plastic sheet. Relative permittivities $\varepsilon_{r,bottle}$=2.19 and $\varepsilon_{r,platform}$=3.18 were measured over the frequency range from 800 MHz to 1 GHz for these materials with Agilent VNA E8358A, using Agilent 85070E dielectric probe kit. In the simulations, both the plastic bottle and the antenna platform were modeled as low loss dielectrics with a loss tangent of 0.005.

An important initial observation that steered the design towards the prototype presented below was that by bending a center-fed dipole antenna onto a plastic cylinder ($\varepsilon_{r,bottle}$=2.19) filled with water, the nulls from the dipole E-plane pattern can be removed by an appropriate choice of the dipole length. Another key-observation was that with a fixed dipole length, which provided the omnidirectional pattern, the best radiation efficiency was achieved with a narrow dipole width. These two observations are exemplified in Fig. 1.

After these initial observations, modifications of the simple straight dipole were studied to find appropriate antenna geometry to produce the desired radiation properties together with good conjugate impedance matching with the tag chip. The design metrics used was the tag read range (d_{tag}) given by

$$d_{tag} = \frac{\lambda}{4\pi}\sqrt{\frac{\tau G_{tag}\,\mathrm{EIRP}}{P_{ic,0}}}, \quad \text{with} \quad \tau = \frac{4\,\mathrm{Re}(Z_{tag})\mathrm{Re}(Z_{ic})}{\left|Z_{tag}+Z_{ic}\right|^2}, \qquad (1)$$

where G_{tag} is the tag antenna gain, EIRP is the equivalent isotropically radiated power (limited by the local radio regulations), and τ is the power transmission coefficient between the tag antenna and tag chip impedances Z_{tag} and Z_{ic}, respectively. The prototype tag is equipped with the Higgs-3 EPC Generation 2 UHF RFID IC by Alien Technology with the chip sensitivity $P_{ic,0}$=−18 dBm. In the current design, the measured tag chip impedance at the chip sensitivity level reported by Björninen et al. [7] was used. The frequencies considered and the corresponding EIRP values are listed in Table I.

Table I. The design frequencies and the corresponding EIRP values. [8]

Region	EU	US	Japan
f [MHz]	866.6	915	954.2
EIRP [W]	3.18	4	4

In the present application, the achievable radiation efficiency of the antenna on the bottle is severely limited by the vicinity of the water. With a simple straight dipole antenna, this results to very low input resistance. However, as a folded dipole can potentially have high input impedance compared with a straight dipole with the same length [9], the folded dipole geometry was considered advantageous for the current design. Moreover, to be able to easily wrap the tag antenna onto the water bottle, the antenna foot print size is limited to approximately that of the traditional product label placed at the smooth cylindrical section of the bottle. Since the achievable radiation efficiency is proportional to the electrical size of the antenna, it is favorable to try to make use of the available space

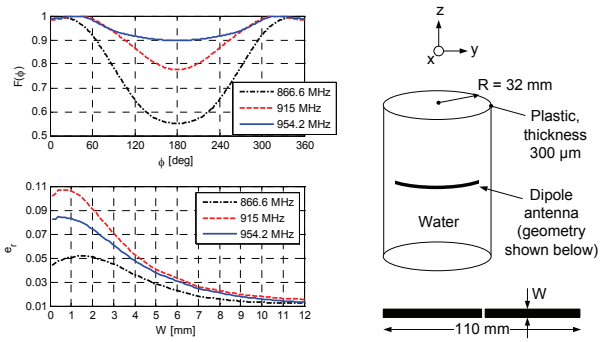

Fig. 1. Top left: simulated normalized power (normalization to the maximum value over all spatial directions) pattern of a dipole with W=1 mm in the xy plane. Bottom left: simulated radiation efficiency of the dipole versus the dipole width.

as much as possible. Taking into account that using a wide antenna conductor did not increase the radiation efficiency in the initial studies (see Fig. 1), the selection of the antenna geometry converged to a three-wire antenna with up to 3 mm trace width, occupying the area of a traditional product label. In addition, simulations showed that open-circuiting the two folded dipole arms in the middle and bending them inward is favorable for the radiation efficiency, but had only a minor effect on the other antenna properties. Thus the impedance matching and final tuning of the antenna shape was done with the antenna geometry shown in Fig. 2.

The impedance matching between the tag antenna and the tag chip was done with the embedded T-matching approach based on shorting the antenna terminals near the tag chip with a conductor loop. In this way the capacitive input impedance of a short dipole can be transformed to inductive and the input reactance of a fixed-length T-matched antenna is controlled by the size of the shorting loop [10]. To preserve the symmetry of the antenna structure, the T-matching loop was placed on both sides of the tag chip. Finally, the built-in genetic optimizer of the HFSS version 12 was employed to select appropriate shape of the antenna and the T-matching loop to achieve a minimum two-meter read range around the water bottle, at all three

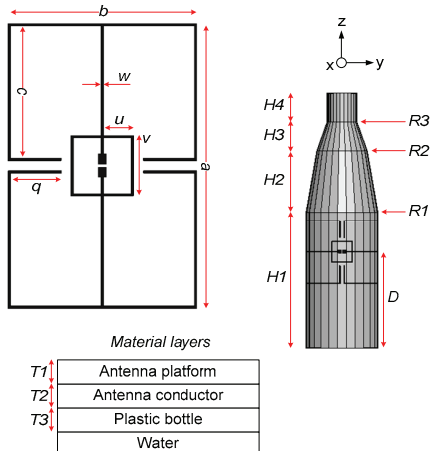

Fig. 2. The simulation model and the associated parameters.

Table II. Values of the model parameters in millimeters.

a	*b*	*c*	*u*	*v*	*w*	*D*
87.8	57.9	41.9	9.2	18.9	0.75	86.5
q	*H1*	*H2*	*H3*	*H4*	*R1*	*R2*
15.6	123	56	26	26	32	22.3
R3	*T1*	*T2*	*T3*			
13.3	0.125	0.025	0.3			

Table III. Simulated radiation efficiency and gain of the tag antenna in the direction of the positive x-axis in Fig. 2.

f [MHz]	866.6	915	954.2
e_r	0.065	0.076	0.079
G_{tag} [dBi]	−9.7	−10.8	−10.3

design frequencies. The simulation model and the associated parameter values are shown in Fig. 2 and the numerical values of these parameters are listed in Table II. The optimization was done first for parameters *a*, *b* and *w* to achieve an omnidirectional pattern with maximal radiation efficiency and afterwards for parameters *u* and *v* to arrange good conjugate impedance matching with the tag chip.

As design metrics the read range of the tag is very descriptive, but since the EIRP in equation (1) is only defined at certain frequencies, the realized tag antenna gain, given by $G_{r,tag}=\tau G_{tag}$, is a preferred quantity to verify the frequency response of the tag over a wide range of frequencies. It is a fundamental tag performance quantity, which combines the radiation properties of the tag antenna with the impedance matching. The effective aperture of the tag antenna ($A_{e,tag}$) and thereby the delivered power to the tag chip (P_{ic}) are also determined by the realized tag antenna gain through

$$\tau A_{e,tag} = \frac{\lambda^2 G_{r,tag}}{4\pi}, \quad P_{ic} = \tau A_{e,tag} S_{inc}, \tag{2}$$

where S_{inc} is the incident power density at the tag's location.

The simulated tag antenna impedance and the conjugate of the measured tag chip impedance reported by Björninen et al. [7] are shown in Fig. 3. These two quantities determine the power transmission coefficient (τ) in equation (1). For comparison between the simulated and measured frequency response of the tag, the simulated realized tag antenna gain

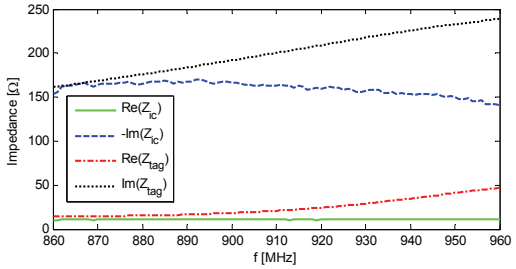

Fig. 3. Simulated antenna impedance and the conjugate of the tag chip impedance [7].

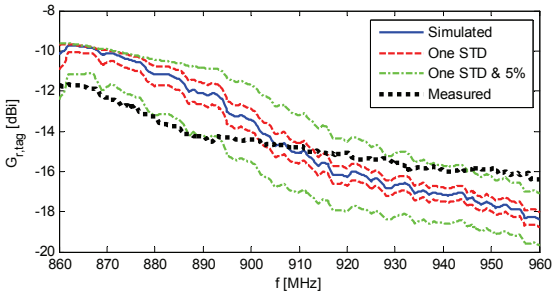

Fig. 4. Simulated and measured realized tag antenna gain in the direction of the positive x-axis in Fig. 2 and the associated uncertainty envelopes.

from 860 MHz to 960 MHz is presented in Fig. 4. The corresponding simulated radiation efficiencies and gains at the design frequencies are listed in Table III. In addition, the simulated read range of the tag around the bottle in the xy-plane of Fig. 2, is shown in Fig. 5. In this plane cut, the tag antenna is linearly polarized with diminishing z-directed field components and simulated axial ratio value greater than 24 dB. The results in Figs. 4-5 also include two uncertainty envelopes corresponding to one standard deviation (STD) uncertainty in tag chip resistance and reactance, and this uncertainty combined with a maximum 5% error in the simulated tag antenna resistance and reactance. The uncertainty envelopes help to quantify the design uncertainties.

III. Tag Measurements And Discussion

Measuring the tag read range directly by taking the tag farther away from the reader antenna until its response stops has the disadvantage that the reflections from the surroundings may affect the outcome. Conducting this measurement in an anechoic chamber avoids this problem, but since the anechoic chambers are often limited in size, an alternative method based

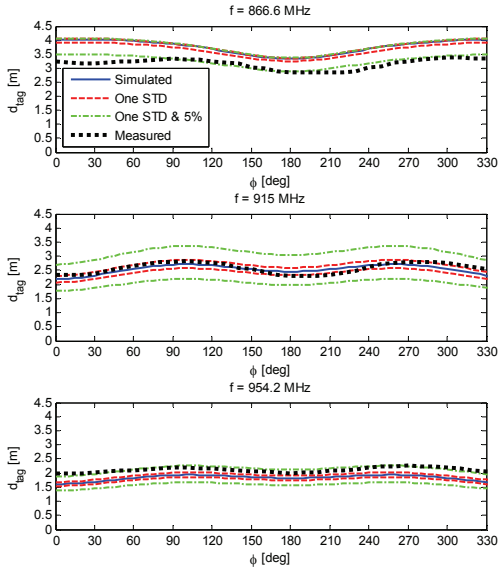

Fig. 5. Simulated and measured read range patterns of the tag in the xy plane in Fig. 2 with the associated uncertainty envelopes.

on the ramping of the transmitted power is advantageous. In this way, also higher repeatability and accuracy are achieved, since neither the tag nor the reader antenna needs to be moved during the measurement.

To obtain the read range and the realized gain of the tag antenna using the power ramping method, the EPC Generation 2 *query* command (to which the tag replies with its identification code) was sent to the tag under test, while illuminating it with a decreasing carrier power density. The measured quantity was the threshold power (P_{th}), defined as the minimum transmitted carrier power, which enables a valid response from the tag. The measurement was conducted in a compact anechoic chamber with Tagformance measurement device [11], which is a measurement unit for RFID tag performance characterization. It allows power ramping at a defined frequency and thereby the threshold power analysis. The core operations of the device are performed with a vector signal analyzer. Using a calibration tag provided by the device manufacturer, the measurement environment was also characterized in terms of the measured pathloss (L_{fwd}) from the generator's output port to the input port of a hypothetic isotropic antenna placed at the tag's location. With this procedure, any possible multipath propagation in the measurement environment is further suppressed. Using these measured data, the maximum line of sight read range and realized tag antenna gain are calculated with

$$d_{tag} = \frac{\lambda}{4\pi}\sqrt{\frac{\mathrm{EIRP}}{L_{fwd}P_{th}}} \quad \text{and} \quad G_{r,tag} = \frac{P_{ic,0}}{L_{fwd}P_{th}}, \tag{3}$$

respectively. These quantities are presented in Figs. 4-5.

The simulated tag antenna impedance in Fig. 3 suggests good impedance matching with the tag chip at the European RFID frequencies. It is also observed that the impedance mismatch is increasing with frequency while the simulated tag antenna gain, shown in Table III, remains nearly constant. As a result, the frequency-slope of the realized tag antenna gain, shown Fig. 4, is negative. This prediction agrees with measured realized gain, which is also shown in Fig. 4. Comparing the two uncertainty envelope presented in this figure, reveals that the accuracy of the simulation model is crucial since combining the simulation uncertainty together with the uncertainty based on the tag chip impedance uncertainty alone, results in a much broader envelope. The measured realized gain is within this envelope at a 60 MHz band in the middle of the studied frequency range and in general the frequency trends of the simulated and measured responses agree well. This adds assurance to the obtained results and shows that the simulation model used in the design is well applicable in practical designs.

As seen from equation (1), the read range of the tag is proportional to the square root of the realized gain. Therefore, compared with the realized tag antenna gain, the read range of the tag is decreasing more gradually with the frequency and it is still reasonable at the highest design frequency 954.2 MHz, as seen from Fig. 5. The results in Fig. 5, also verify the important design goal: omnidirectional radiation pattern around the bottle. Furthermore, a minimum two-meter read range, which is sufficient for many applications, was measured around the bottle at all three design frequencies.

IV. Conclusions And Future Work

The development of a low profile and low cost conformal tag antenna for identification of water bottles with passive UHF RFID has been discussed. The developed tag antenna does not contain any material layer in between the tag antenna conductor and the bottle and it could therefore be directly manufactured onto the bottle to avoid additional material costs. An accurate representation of the water bottle was implemented in a full-wave electromagnetic simulator to co-design the tag antenna with the water bottle. Comparison between the simulation and measurement results verified that the simulation model is well applicable in practical designs. When mounted on the plastic bottle filled with water, the developed tag antenna has an omnidirectional radiation pattern in the plane normal to the bottle axis with the maximum line of sight read range more than two meters at the European, US and Japanese UHF RFID frequencies.

The achievable radiation efficiency in the vicinity of water severely limits the readable range of the tag. The future work includes investigation of enhancing the radiation efficiency by including a high permittivity material layer in the antenna platform.

References

[1] A. Lehto, J. Nummela, L. Ukkonen, L. Sydänheimo, and M. Kivikoski, "Passive UHF RFID in paper industry: challenges, benefits and the application environment," *IEEE Trans. Autom. Sci. Eng.*, vol. 6, no. 1, pp. 66–79, Jan. 2009.

[2] J. Virtanen, L. Ukkonen, T. Björninen, and L. Sydänheimo, "Printed humidity sensor for UHF RFID systems," *proceedings of the IEEE Sensors Applications Symposium (SAS)*, pp. 269-272, Feb. 23-25, Limerick, Ireland, 2010.

[3] T. Kellomäki, T. Björninen, L. Ukkonen, and L. Sydänheimo, "Shirt collar tag for wearable UHF RFID systems," *proceedings of the Fourth European Conference on Antennas and Progation*, pp. 1-5, Apr. 12-16, Barcelone, Spain, 2010.

[4] C. Occhiuzzi, S. Cippitelli, and G. Marrocco, "Modeling, Design and Experimentation of Wearable RFID Sensor Tag," *IEEE Trans. Antennas Propag.*, vol. 58, no. 8, pp. 2490-2498, Aug. 2010.

[5] H. Rajagopalan, Y. Rahmat-Samii, "Platform Tolerant and Conformal RFID Tag Antenna: Design, Construction and Measurements," *Journal of the Applied Computational Electromagnetics Society (ACES)*, vol. 25, no. 6, pp. 486-497, June 2010.

[6] W. J. Ellison, K. Lamkaouchi, and J.-M. Moreau, "Water: a dielectric reference," *Journal of Molecular Liquids*, vol. 68, no. 2-3, pp. 171-279, Apr. 1996.

[7] T. Björninen, M. Lauri, L. Ukkonen, L. Sydänheimo, A. Elsherbeni, and R. Ritala, "Wireless Measurement of UHF RFID Chip Impedance," *proceedings of the 32nd Annual Antenna Measurement Techniques Association (AMTA) Symposium*, pp. 35-40, Oct. 10-15, Atlanta, Georgia, USA, 2010.

[8] EPCglobal Frequency Regulations UHF: http://www.epcglobalinc.org/tech/freq_reg/

[9] W. L. Stutzman, G. A. Thiele, *Antenna Theory and Design*, John Wiley & Sons, Inc., 1981.

[10] G. Marrocco, "The art of UHF RFID antenna design: impedance-matching and size-reduction techniques," *IEEE Antennas Propag. Mag.*, vol. 50, no. 1, pp. 66-79, Feb. 2008.

[11] Voyantic Ltd., Espoo, Finland: http://www.voyantic.com/